A Study on the Shielding for Wireless Charging Systems of Electric Vehicles

Hongzhi Cui, Wenxing Zhong, Hao Li, Fengchun He, Min Chen and Dehong Xu
Institute of Power Electronics
Zhejiang University
Hangzhou 310027, China
xdh@cee.zju.edu.cn

***Abstract*—With a high power level and a large transfer distance in a wireless charging system of electric vehicles, human exposure to electromagnetic filed becomes a major concern. In this paper, some key parameters of an aluminum plate and ring shield are studied with the aid of finite-element analysis. The shielding effectiveness and the power transfer efficiency are investigated simultaneously as one of the parameters changes. It is found that the shielding effect mainly depends on the size of the shield while increasing the distance between the shield and the ferrite layer attenuates efficiency drop due to the eddy-current loss in the shield. A 3.3kW wireless charging system with 20cm air gap was built to verify the simulation results.**

Keywords—electric vehicles; wireless power transfer; electromagnetic field; electromagnetic shielding;

I. INTRODUCTION

Nowadays, energy and environment issues have drawn more and more attention. With advantages of high energy efficiency and zero emission, the electric vehicle (EV) gains increasingly attention. However, the relatively low energy density of the battery constrains the travel distance of an EV. Besides, frequently plugging in and off the car charger may upset an EV user. Wireless power transfer (WPT) technology is considered as an effective way to solve this problem. With WPT technology, an electric vehicle is able to achieve opportunity charging [1]. For example, by installing wireless charging pads in the park lot even on the road, electric vehicles can be charged more frequently and conveniently. As a result, mile anxiety can be eased. Besides, wireless charger is able to charge a car automatically. The drivers can just park their cars and leave. They will never have the trouble of forgetting to charge. In addition, without cable, wireless charger is much safer and can adapt to severe weather [2].

The most common way to realize WPT at present is inductive power transfer technology, which consists of a transmitting coil and a receiving coil. Through electromagnetic field (EMF), the power can be delivered wirelessly. Recent research has been undergoing with respect to power transfer efficiency, adaptability to misalignment, and distance etc. [3]-[8]. However, with the increase of power level and air gap distance, the electromagnetic field generated around the system should also be a concern. According to the most referred guidelines published by the international commission on non-ionizing radiation protection (ICNIRP) in 2010, the reference level for general public is 27μT at frequency ranging from 3kHz to 10MHz, which covers most of the operation frequency of a WPT system for EVs [9]. As a result, when designing a WPT system, proper shielding methods should be utilized to fulfill this standard.

In general, there are passive and active shielding methods to eliminate EMF. For passive methods, ferromagnetic materials are used as magnetic flux guide to constrain the EMF. Conductive materials such as aluminum are used to shield EMF. Utilizing ferromagnetic materials has benefit to improving magnetic coupling between the coil pads and improves system efficiency. However, ferromagnetic materials are usually fragile and expensive. Besides, in some circumstances, only using ferromagnetic materials may fail to constrain the EMF under the standard. As a result, conductive materials are often used as an auxiliary measure in practice. Effective cancellation of the electromagnetic field is found in [10] by combining those two methods. Similar to using conductive materials as shields, a resonant reactive shielding method was proposed in [11]. By using a passive compensation loop coil with a capacitor for resonance, this method demonstrates more effective shielding effect than a conductive shield with the same size. As for active methods, counter current is generated deliberately to achieve EMF cancellation. Active shielding methods may be used in the case of high power, large air gap and low magnetic coupling, where the passive shielding method is insufficient. [12]. Usually, passive shielding methods are preferred because they are simple, and cost effective.

Several factors should be considered when designing WPT shields. This paper investigates how the parameters of an aluminum plate and an aluminum ring affect the EMF and the performance of a WPT system. The investigation is organized into five sections. Section II starts with the setup of the WPT system. The research method and some key parameters of the WPT system are introduced. In section III, the simulation results of aluminum plate shield with different size, thickness and distance between the plate and the ferrite layer are presented and discussed. Section IV illustrates the simulation results of aluminum ring shield with different size, width and distance between the ring and the ferrite layer. The results are then compared with aluminum plate shield. In section V a series of experiments are conducted to verify the simulation. Measurements of the dc-dc efficiency and the magnetic field

This work is supported by the Fundamental Research Funds for the Central Universities of China.

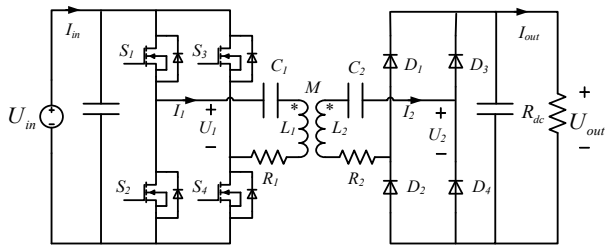

Fig. 1 WPT system overall topology

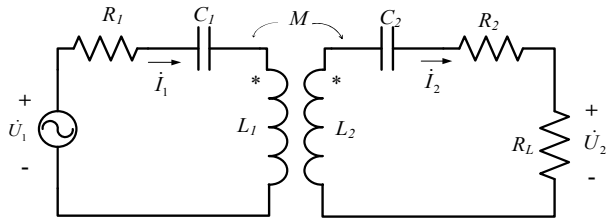

Fig. 2 Equivalent circuit of SS compensation networks

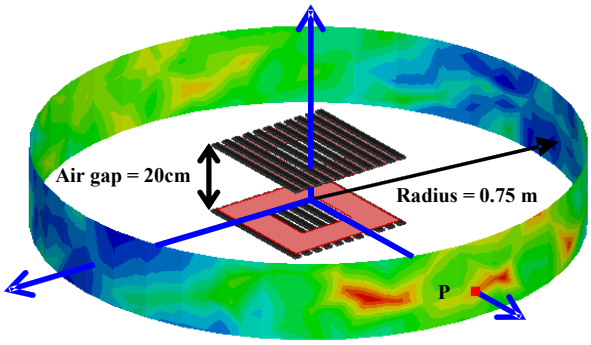

Fig. 3 Schematic of the WPT system and the observation spot.

density with 3.3kW output power are presented. Finally, in section VI, the investigation results are summarized.

II. Setup of the WPT System

A 3.3 kW WPT system was built to investigate the shielding effect. Fig. 1 shows the overall topology of this system, which consists of a high frequency inverter, a power delivery coil with its compensation networks and a full bridge rectifier. Conventional series-series (SS) compensation networks are adopted. According to the standard SAE-J2954, the operating frequency f_o of an EV charging system should be within the range of 81.39 – 90 kHz and center at 85 kHz. The output voltage and output current is assumed constant in order to compare the effect of different shields. The equivalent circuit of SS compensation networks is shown in Fig. 2, where L_1 and L_2 are the self-inductance of the primary side and secondary side respectively. C_1 and C_2 are the compensation capacitors. M is the mutual inductance between the primary coil and the

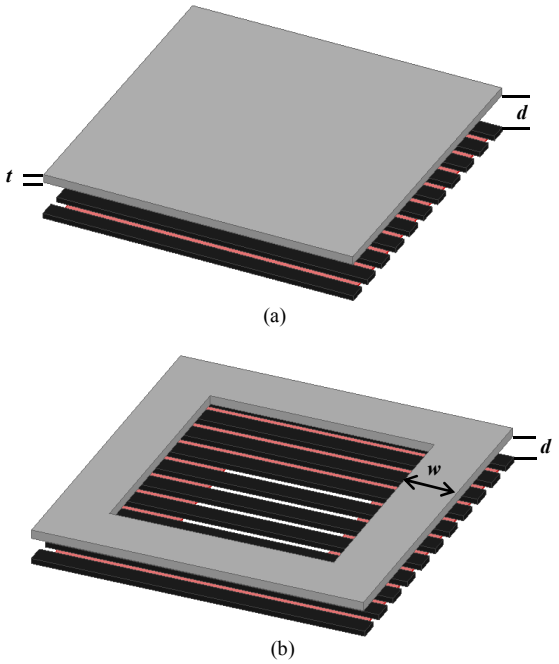

Fig. 4 Shields used in the simulation: (a) aluminum plate; (b) aluminum ring

TABLE I Geometric Parameters of the Coils

Parameter	Value
Coil edge length	350 mm
Ferrite bar length	370 mm
Ferrite bar width	20 mm
Ferrite bar thickness	6 mm
Num. of ferrite bars in total	22
Air gap	20 cm

secondary coil. R_1 and R_2 are the parasitic resistance of the coil plus the equivalent series resistance of the capacitor. R_L is the equivalent load resistance of the rectifier. Based on the analysis in [13], R_L can be expressed as

$$R_L = \frac{8}{\pi^2}\frac{U_{out}^{\ 2}}{P_o} \tag{1}$$

where U_{out} is the output dc voltage of the rectifier and P_o is the output power. According to the fundamental wave analysis method, the following equations can be obtained [14].

$$\begin{bmatrix} \dot{U}_1 \\ 0 \end{bmatrix} = \begin{bmatrix} \mathrm{j}(\omega L_1 - \frac{1}{\omega C_1}) + R_1 & \mathrm{j}\omega M \\ \mathrm{j}\omega M & R_L + R_2 + \mathrm{j}(\omega L_2 - \frac{1}{\omega C_2}) \end{bmatrix} \begin{bmatrix} \dot{I}_1 \\ \dot{I}_2 \end{bmatrix} \tag{2}$$

Both the primary side and the secondary side are resonant at the operating frequency. Then the current of the secondary side I_2 and the primary side I_1 can be expressed as

$$|\dot{I}_2| = \sqrt{\frac{P_o}{R_L}} \tag{3}$$

$$|\dot{I}_1| = \frac{(R_L + R_2)}{2\pi f_o M} |\dot{I}_2| \tag{4}$$

It should be noticed that the added aluminum shield will increase R_2 and reduce M. Thus two simulations are required to get a precise result for each set of parameters. The first simulation will use arbitrary coil currents and obtain the values of R_2 and M of the coil with the shield. The values can then be substituted into (4) to calculate the required primary current for generating a rated output current at 3.3kW. I_1 and I_2 are then used in the second simulation to get the results of the interested parameters.

The structure of the coils used in this system is shown in Fig. 3 and the geometric parameters of the coils are listed in TABLE I. It is assumed that the width of a car is around 1.5 m. The magnetic flux density of the place 0.75 m away from the center of the coils is observed, as illustrated in Fig. 3. The magnetic flux density is maximized at point P due to the orientation of the magnetic bars. Therefore it is selected as the field observation spot in the following simulations and experiments. Fig. 4 shows the aluminum shields under investigation. The aluminum shield size, distance between the shield and the ferrite layer d, aluminum plate thickness t and ring width of the aluminum ring plate w are investigated.

III. Simulation Study of Using Aluminum Plate as a Shield

A. Size of the Aluminum Plate

Fig. 5 shows the simulation results of different aluminum plate sizes. In the simulation, the plate shield thickness t is 4 mm and the distance d between the plate and the ferrite layer is 4 mm. The horizontal axis is the ratio of the aluminum plate edge length to the ferrite bar length, which indicates the size of the shield. The normalized B-field is the ratio of the magnetic flux density at point P to that when without shielding. It can be seen that as the size of the aluminum plate increases, the core loss and coil loss increase while the coupling coefficient k drops dramatically as shown in Fig. 5(a). Meanwhile, the B-field at point P and coil efficiency also decrease with increase of the shield size as shown in Fig. 5(b) . The B-field at point P is reduced by half when the normalized shielding plate size increases to 1.25. When the normalized size is more than 1.25, the increment of plate size has no significant effect on either shielding effect or the power transfer efficiency.

B. Thickness of the Aluminum Plate

Fig. 6 shows the simulation results of different aluminum plate thickness t. In the simulation, the plate normalized size is 1 and the shield to ferrite distance d is 4 mm. It can be seen that the plate thickness t has little effect on the core loss, coil loss, coupling coefficient and magnetic flux strength. However, when the plate thickness is smaller than 5mm, the plate loss

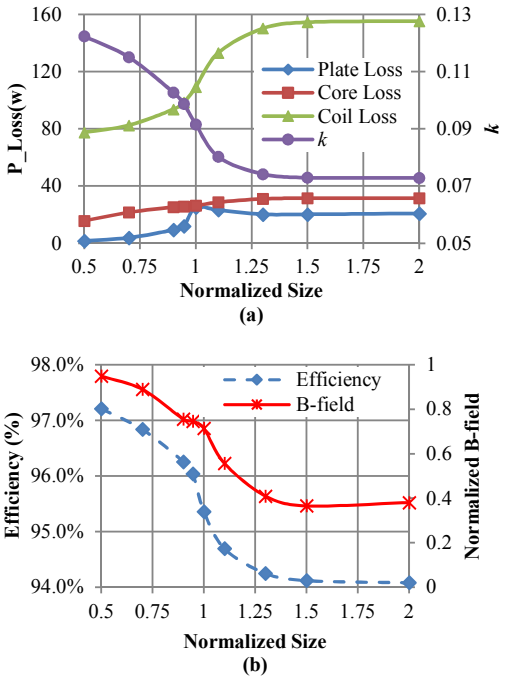

Fig. 5 Simulation results of different aluminum plate sizes: (a) plate loss, core loss, coil loss and coupling coefficient k; (b) coil efficiency and normalized B-field.

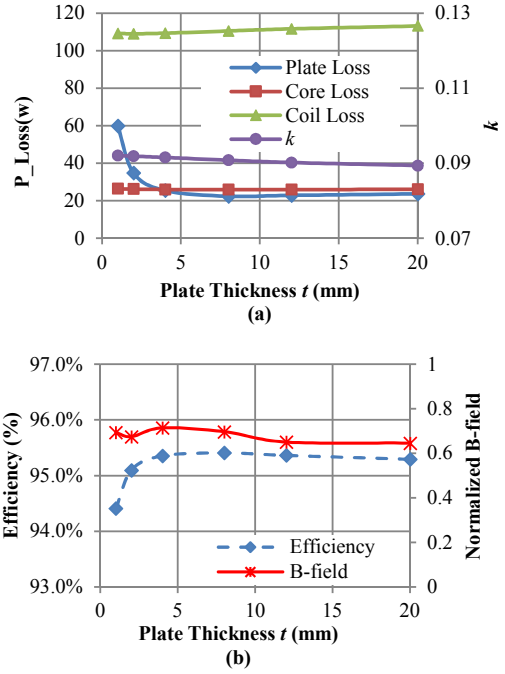

Fig. 6 Simulation results of different aluminum plate thicknesses: (a) plate loss, core loss, coil loss and coupling coefficient k; (b) coil efficiency and normalized B-field.

demonstrates a sharp increase as the thickness is further reduced, which will degrade the power transfer efficiency. As a result, there is an lower limit for plate thickness for obtaining higher

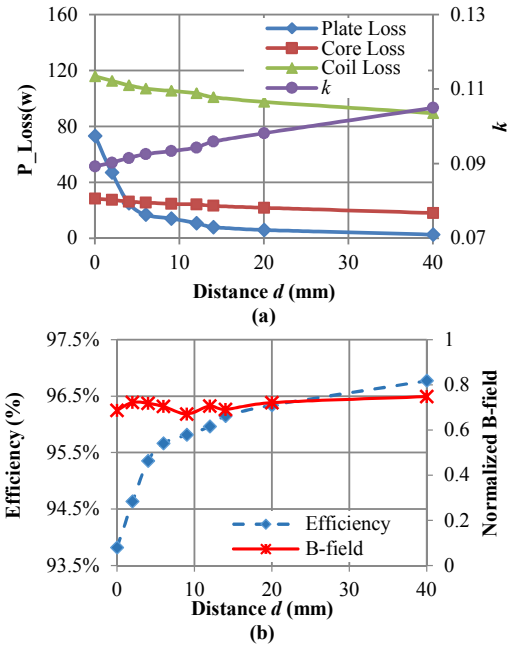

Fig. 7 Simulation results of different distances between the aluminum plate and the ferrite layer: (a) plate loss and core loss, coil loss and coupling coefficient *k*; (b) coil efficiency and normalized B-field.

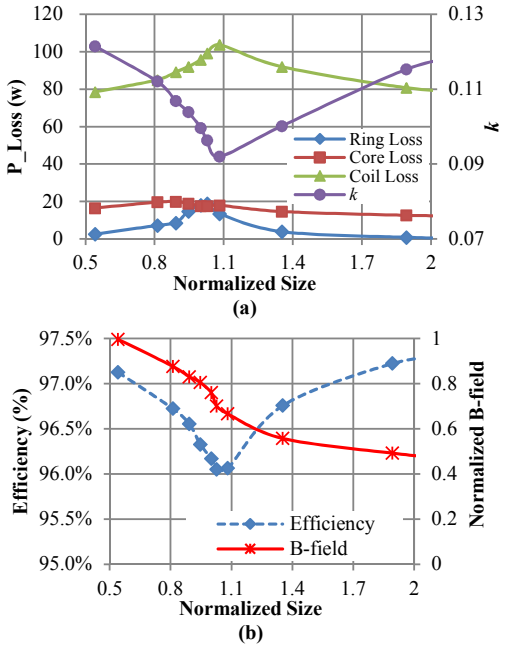

Fig. 8 Simulation results of different aluminum ring sizes: (a) plate loss and core loss, coil loss and coupling coefficient *k*; (b) coil efficiency and normalized B-field.

efficiency. Therefore, when using aluminum plate as a shield, the plate thickness needs to be properly designed. Thicker plate has little benefit to shielding. However it will increase weight of the charging pad.

C. Distance between the Aluminum Plate and Ferrite layer

Fig. 7 shows the simulation results of different distance *d* between the plate and ferrite layer. In the simulation, the normalized size of the plate is 1 and the shield thickness *t* is 4 mm. It can be seen that as the distance between the plate and ferrite layer increases, the plate loss, core loss and coil loss are all decreasing. When the distance *d* is within 10 mm, the shielding plate loss drops quickly with the increment of the distance. In the meantime, the magnetic field density almost remains unchanged. That is because the coupling coefficient *k* will increase as the distance is enlarged, which contributes to a lower electromagnetic radiation. According to the simulation, when the plate to ferrite distance *d* increases from 0 mm to 20 mm, the coil efficiency increases 2.5 percentage while the magnetic flux density only increases 5%. Therefore, when designing an aluminum plate shield, it is recommended to increase the distance between aluminum plate and ferrite layer moderately if volume is allowed. It may enlarge the volume of the pad slightly but the coil efficiency will rise. Besides, the shielding effect and the pad weight are almost unchanged.

IV. Simulation Study of Using Aluminum Ring as a Shield

A. Size of the Aluminum Ring

Fig.8 shows the simulation results of different aluminum ring size. In the simulation, the ring width *w* is 15 mm and the distance *d* between the ring and the ferrite layer is 4 mm. It can be seen that the magnetic field density decreases as the ring size increases, and the dropping rate starts to decrease when the normalized size is larger than 1.3 which is similar to the case of using aluminum plate. However, the efficiency curve of the system turns out to be "V" shape. When the normalized ring size is 1.5, the normalized B-field is about 0.52 and the coil efficiency is about 96.9%, compared with a normalized plate size of 1.1 and an efficiency of 96.2% when achieving a similar normalized B-field in the case using aluminum plate. Therefore, ring shape shield shows superior efficiency performance compared with plate shield but the size of the shielding ring needs to be larger than the shielding plate in order to achieve similar magnetic field attenuation.

B. Aluminum Ring Width

The simulation results of different aluminum ring width *w* are shown in Fig.9. In the simulation, the normalized size is 1 and the distance *d* between the ring and the ferrite layer is 4 mm. The results are similar to that of the case investigating the effect of aluminum plate thickness *t*. When the ring width is smaller than 5 mm, with the increment of ring width, the ring loss will decrease dramatically, which leads to the enhancement of coil efficiency. However, if the ring width increases further, the dropping coupling coefficient will result in the increment of the primary coil current and the coil efficiency will decrease.

C. Distance between the Aluminum Ring and Ferrite Layer

Fig. 10 shows the simulation results of different distance *d* between the ring and the ferrite layer. In the simulation, the normalized size is 1.08 and the ring width *w* is 10 mm. A negative distance implies that the ring overlaps or goes across the ferrite layer in vertical direction. Similar to the results of

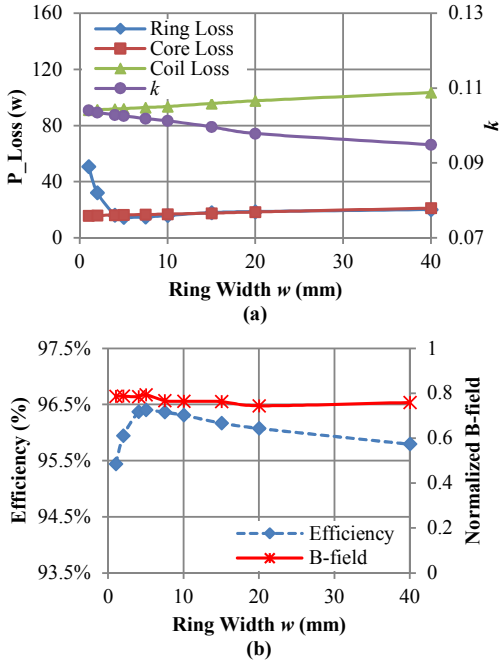

Fig. 9 Simulation results of different aluminum ring widths: (a) plate loss and core loss, coil loss and coupling coefficient k; (b) coil efficiency and normalized B-field.

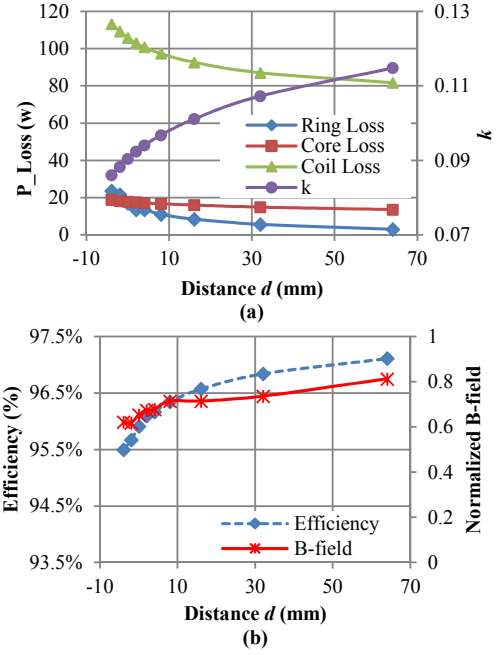

Fig. 10 Simulation results of different distances between the aluminum ring and ferrite bars: (a) plate loss and core loss, coil loss and coupling coefficient k; (b) coil efficiency and normalized B-field.

plate, increasing the distance moderately can enhance the coupling and improve the coil efficiency while remain the shielding effectiveness.

(a)

(b)

Fig. 11 Couplers of the WPT system: (a) with aluminum plate shield; (b) with aluminum ring shield.

V. Experiment Validation

Experiments are carried out to verify the simulations. A 3.3 kW wireless charging system for electric vehicles has been built for practical measurements. Fig. 11 shows the setup of the system which has the same structure and geometric parameters as shown in Fig. 4 and TABLE I, respectively. Litz wire with strand diameter of 0.1 mm and 300 strands is used to minimize the skin effect. The output power of the system is 3.3 kW, the dc output voltage is 317 V and the operation frequency is 83.9 kHz. The dc-dc efficiency of the system and the magnetic field density at point P are measured and compared with the simulation results. The dc-dc efficiency is measured with PM6000 power analyzer from Voltech. The magnetic field density is measured with ESRP EMI test receiver from ROHDE&SCHWARZ and the RMS value of the magnetic field density is 10.8μT at point P without shielding.

TABLE II EXPERIMENT CONDITIONS OF ALUMINUM PLATE SHIELD

Investigated Parameter	Normalized Size	Thickness *t*	Distance *d*
Size	-	4mm	14mm
Thickness *t*	1	-	4mm
Distance *d*	1	4mm	-

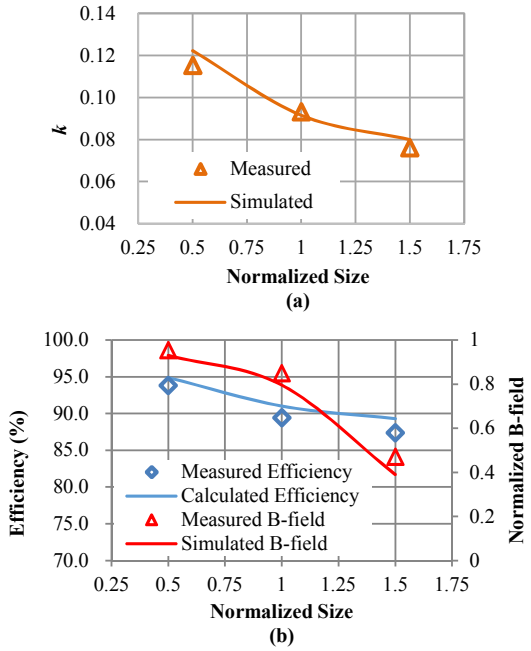

Fig. 12 Experimental results of different plate sizes: (a) coupling coefficient *k*; (b) dc-dc efficiency and normalized B-field.

A. Using aluminum plate as a shield

The shielding effect of aluminum plate is firstly investigated. The effect of three parameters, i.e. plate size, plate thickness and plate-to-ferrite distance, is studied. The experiment conditions are listed in TABLE II. The experimental results of different plate size are shown in Fig. 12. It can be seen that the experimental results are consistence with the simulations. B-field at point P changes obviously with different plate sizes. When the normalized plate size increases from 0.5 to 1.5, the normalized B-field decreases from 0.95 to 0.47. However, the efficiency of the system will also decrease with a larger plate. The coupling coefficient drops from 0.12 to 0.076 as shown in Fig. 12 (b) which accounts for the reduction of the dc-dc efficiency from 93.83% to 87.38%.

The experimental results of different plate thickness *t* are shown in Fig. 13. It can be seen that plate thickness has little effect on the shielding effect as well as the system efficiency. However, the plate thickness should be larger than some critical value, otherwise the system efficiency will be deteriorated. As shown in Fig. 13 (b), the measured efficiency at thickness 4mm has an obvious decrease compared with that at 8mm.

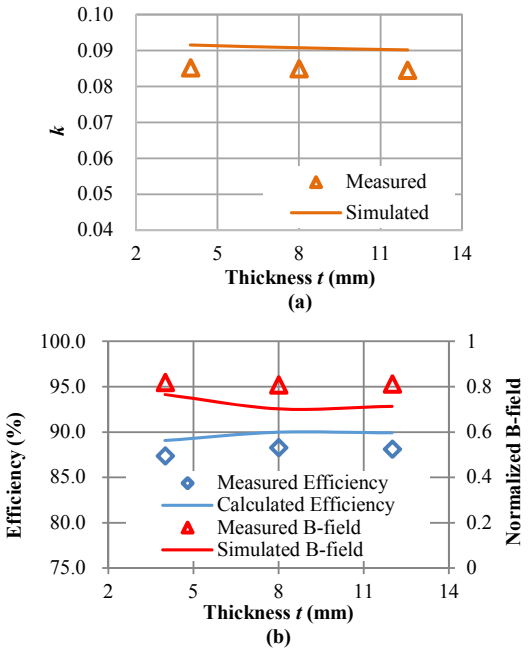

Fig. 13 Experimental results of different plate thicknesses: (a) coupling coefficient *k*; (b) dc-dc efficiency and normalized B-field.

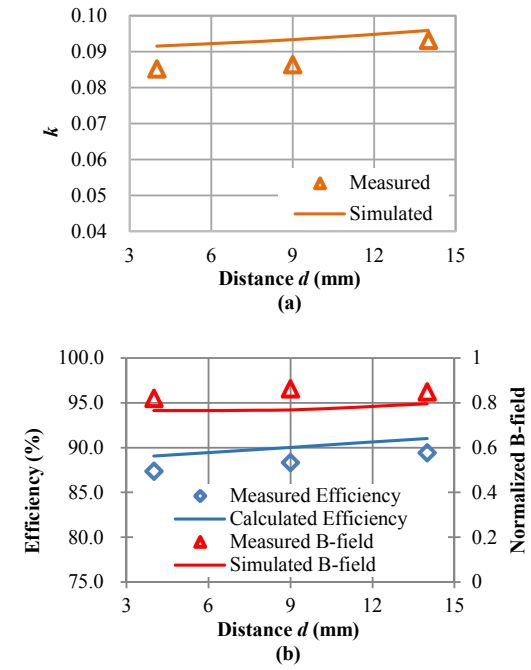

Fig. 14 Experimental results of different plate-to-ferrite distances: (a) coupling coefficient *k*; (b) dc-dc efficiency and normalized B-field.

TABLE III EXPERIMENT CONDITIONS OF ALUMINUM RING SHIELD

Investigated Parameter	Normalized Size	Width *w*	Distance *d*
Size	-	4mm	14mm
Width *w*	1	-	4mm
Distance *d*	1	15mm	-

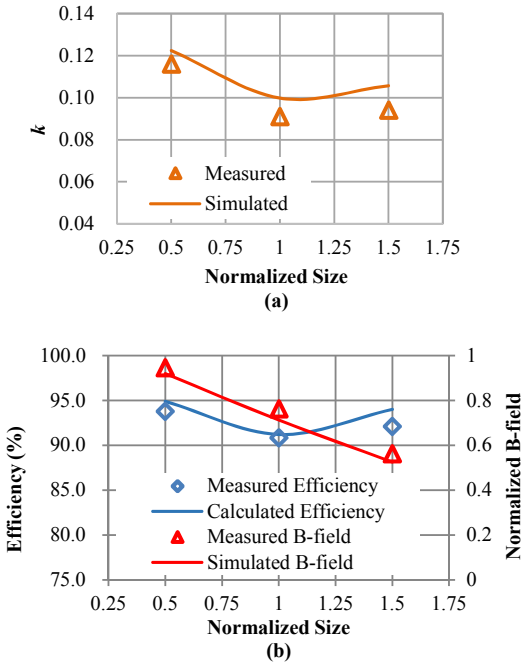

Fig. 15 Experimental results of different aluminum ring sizes: (a) coupling coefficient *k*; (b) dc-dc efficiency and normalized B-field.

Fig. 14 shows the experimental results of different plate-to-ferrite distance *d*. It can be seen that increasing the distance can weaken the effect of the plate on the coupling coefficient *k*. Therefore, with a larger distance, the system efficiency is improved. As shown in Fig. 14 (b), when the distance is enlarged from 4 mm to 14 mm, the measured dc-dc efficiency increases by 2%. Meanwhile, the B-filed at point P only has a small increase. However, the volume of the receiver will be limited in a real application and therefore the plate-to-ferrite distance can only vary in a small range.

B. Using aluminum ring as a shield

The effect of an aluminum ring on shielding as well as system efficiency are practically studied. The experiment conditions are listed in TABLE III. Fig. 15 shows the experimental results of different ring size. It can be seen that as the ring size increases, the B-field at point P decreases and the efficiency curve has a "V" shape. The measured dc-dc efficiency reaches the minimum value when the normalized size is 1. Therefore, when using aluminum ring as a shield, the normalized ring size should exceed 1 so that a higher system efficiency and a better shielding can be achieved. Compared with aluminum plate, the dc-dc efficiency with aluminum ring shield is higher when achieving similar shielding effect but the required ring size is larger than the plate size.

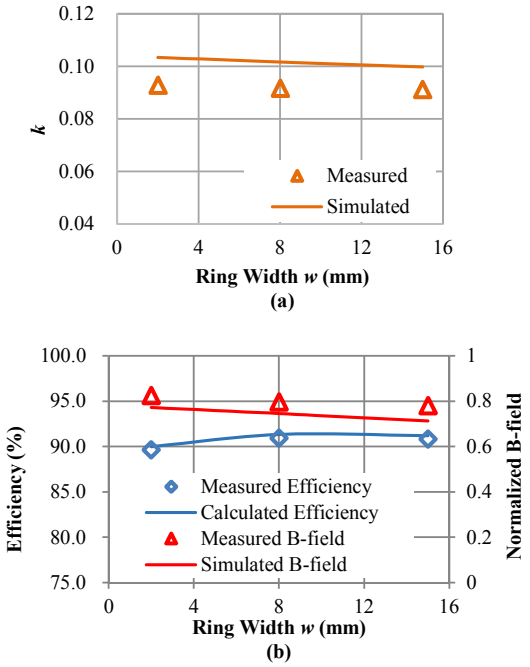

Fig. 16 Experimental results of different aluminum ring widths *w*: (a) coupling coefficient *k*; (b) dc-dc efficiency and normalized B-field.

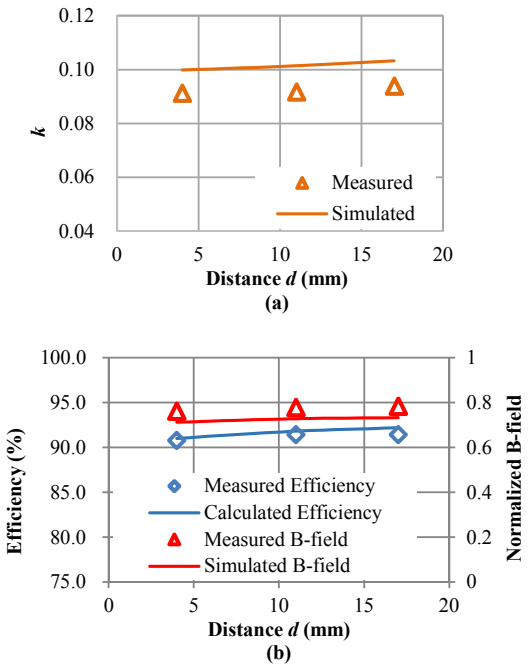

Fig. 17 Experimental results of different distances *d* between the aluminum ring and the ferrite layer: (a) coupling coefficient *k*; (b) dc-dc efficiency and normalized B-field.

Fig. 16 provides the experimental results of different ring width *w*. It can be seen that, the ring width does not affect the B-filed at point P much. However, there is an optimum ring width for high system efficiency. When the ring width increases from

2 mm to 8 mm, the measured dc-dc efficiency increases by 1.3%. Whereas when the ring width *w* is further increased, the measured dc-dc efficiency drops from 90.95% to 90.83%. This is similar to that of the study of the plate thickness. Consequently, when designing the aluminum ring width, the system efficiency rather than the shielding effect should be primarily considered.

The experimental results of different ring-to-ferrite distance *d* are illustrated in Fig. 17. The results are similar to that of the case when using aluminum plate. Increasing the distance will increase coupling coefficient of the coils and push up system efficiency. But the improvements in coupling and efficiency are less obvious compared with the case using aluminum plate. When the ring-to-ferrite distance increases from 4 mm to 17mm, the measured dc-dc efficiency increased by 0.6%.

I. CONCLUSION

In this paper, the shielding effects of aluminum plate and aluminum ring in a WPT system are investigated by FEA simulations and practical measurements. The B-filed at the interested spot can be reduced to about 50% of the value without shielding by using either plate or ring shield. Based on this study, a few design guidelines are provided as follows.

- Size of the shielding plate or ring should be determined by the targeted value of the B-filed;
- There is a minimum thickness of the plate or minimum width of the ring which will provide similar shielding and maintain a high efficiency. Further reducing the thickness of the plate or the width of the ring will cause dramatic decrease in system efficiency.
- The distance between the shield and the ferrite layer should be maximized.
- Ring shape shield is better from the aspects of efficiency and cost.

REFERENCES

[1] S. Lukic and Z. Pantic, "Cutting the cord: static and dynamic inductive wireless charging of electric vehicles," in IEEE Electrification Magazine, vol. 1, no. 1, pp. 57-64, Sept. 2013.

[2] S. Li and C. C. Mi, "Wireless power transfer for electric vehicle applications," in IEEE Journal of Emerging and Selected Topics in Power Electronics, vol. 3, no. 1, pp. 4-17, March 2015.

[3] R. Bosshard, J. Mühlethaler, J. W. Kolar and I. Stevanović, "Optimized magnetic design for inductive power transfer coils," 2013 Twenty-Eighth Annual IEEE Applied Power Electronics Conference and Exposition (APEC), Long Beach, CA, USA, 2013, pp. 1812-1819.

[4] R. Bosshard, U. Iruretagoyena and J. W. Kolar, "Comprehensive Evaluation of Rectangular and Double-D Coil Geometry for 50 kW/85 kHz IPT System," in IEEE Journal of Emerging and Selected Topics in Power Electronics, vol. 4, no. 4, pp. 1406-1415, Dec. 2016.

[5] S. Kim, G. A. Covic and J. T. Boys, "Analysis on tripolar pad for inductive power transfer systems," 2016 IEEE PELS Workshop on Emerging Technologies: Wireless Power Transfer (WoW), Knoxville, TN, 2016, pp. 15-20.

[6] F. Y. Lin, G. A. Covic and J. T. Boys, "Evaluation of magnetic pad sizes and topologies for electric vehicle charging," in IEEE Transactions on Power Electronics, vol. 30, no. 11, pp. 6391-6407, Nov. 2015.

[7] W. Zhong and S. Y. R. Hui, "Reconfigurable wireless power transfer systems with high energy efficiency over wide load range," in IEEE Transactions on Power Electronics, vol. PP, no. 99, pp. 1-1.

[8] Y. Yang, W. Zhong, S. Kiratipongvoot, S. C. Tan and S. Y. R. Hui, "Dynamic improvement of series-series compensated wireless power transfer systems using fiscrete dliding mode control," in IEEE Transactions on Power Electronics, vol. PP, no. 99, pp. 1-1.

[9] ICNIRP Guidelines, "Guidelines for limiting exposure to time-varying electric and magnetic fields (1 Hz to 100 kHz)," Health Phys., vol. 99, no.6, pp. 818–836, 2010.

[10] H. Kim, J. Cho, S. Ahn, J. Kim and J. Kim, "Suppression of leakage magnetic field from a wireless power transfer system using ferrimagnetic material and metallic shielding," 2012 IEEE International Symposium on Electromagnetic Compatibility, Pittsburgh, PA, 2012, pp. 640-645.

[11] S. Kim, H. H. Park, J. Kim, J. Kim and S. Ahn, "Design and analysis of a resonant reactive shield for a wireless power electric vehicle," in IEEE Transactions on Microwave Theory and Techniques, vol. 62, no. 4, pp. 1057-1066, April 2014.

[12] S. Y. Choi, B. W. Gu, S. W. Lee, W. Y. Lee, J. Huh and C. T. Rim, "Generalized active EMF cancel methods for wireless electric vehicles," in IEEE Transactions on Power Electronics, vol. 29, no. 11, pp. 5770-5783, Nov. 2014.

[13] T. D. Nguyen, S. Li, W. Li and C. C. Mi, "Feasibility study on bipolar pads for efficient wireless power chargers," 2014 IEEE Applied Power Electronics Conference and Exposition - APEC 2014, Fort Worth, TX, 2014, pp. 1676-1682.

[14] L. Steigerwald, "A comparison of half-bridge resonant converter topologies," IEEE Trans. Power Electron., vol. 3, no. 2, pp. 174–182, Apr. 1988.